S04030200-TRT10002
ORNL/TM-2022/1828

SECOND TARGET STATION (STS) PROJECT

Generation of Beamline Sources–Preliminary Design

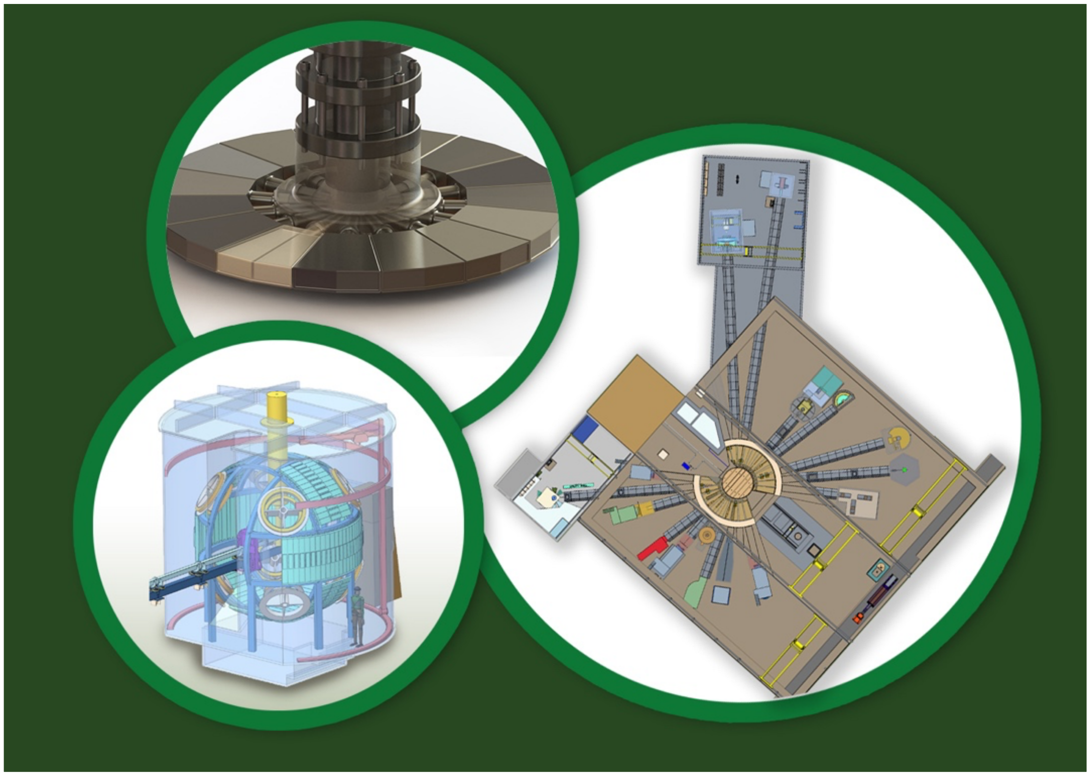

Thomas M Miller
Igor Remec

June 2022

OAK RIDGE National Laboratory

ORNL IS MANAGED BY UT-BATTELLE LLC FOR THE US DEPARTMENT OF ENERGY

S04030200-TRT10002
ORNL/TM-2022/1828

Second Target Station (STS) Project

GENERATION OF BEAMLINE SOURCES–PRELIMINARY DESIGN

Thomas M Miller
Igor Remec

June 2022

Prepared by
OAK RIDGE NATIONAL LABORATORY
Oak Ridge, TN 37831
managed by
UT-BATTELLE LLC
for the
US DEPARTMENT OF ENERGY
under contract DE-AC05-00OR22725

CALCULATION TITLE
STS Project Generation of Beamline Sources–Preliminary Design

LABORATORY ORNL	DIVISION/GROUP Second Target Station (STS) Project	CALC. NO. S04030200-TR10002
Prepared by Thomas M Miller	Level III Manager Igor Remec	Lead Engineer Igor Remec

Other WBS elements affected: None

	Signature/Date			
	REV 0	REV 1	REV 2	REV 3
Prepared by	Thomas M Miller			
Task Leader	Thomas M Miller			
Level III Manager	Igor Remec			
Checked by	Franz Gallmeier			
Lead Engineer	Igor Remec			

CONTENTS

CONTENTS iii
LIST OF FIGURES iv
LIST OF TABLES v
ABBREVIATIONS vi
EXECUTIVE SUMMARY vii
1. SCOPE 1
2. ACCEPTANCE CRITERIA 1
3. ASSUMPTIONS AND LIMITATIONS 1
4. METHODOLOGY AND MODELS 1
5. ANALYSIS AND RESULTS 2
    5.1 GENERATION OF BEAMLINE SOURCES 2
    5.2 EVALUATION OF BEAMLINE SOURCES 7
        5.2.1 Angular Acceptance of the Beamline Sources 8
        5.2.2 Surface Area of the Beamline Sources 11
        5.2.3 Activation 13
6. CONCLUSIONS 15
7. REFERENCES 15
APPENDIX A. COMPUTER HARDWARE AND SOFTWARE A-3
APPENDIX B. LOCATION OF COMPUTATIONAL INPUT AND OUTPUT FILES B-3

LIST OF FIGURES

Figure 1. Overview of a portion of the MCNP model used to calculate the neutron beamline sources. 3
Figure 2. Closer view of the tally surface for the ST11 sources....... 3
Figure 3. Closer view of the tally surface for the ST13 sources....... 4
Figure 4. Spectrum of neutrons entering ST11 and ST13 per source proton. 5
Figure 5. Spectrum of photons entering ST11 and ST13 per source proton. 6
Figure 6. Integral neutron flux below 100 eV at the entrance to each STS beamline. 7
Figure 7. Spectrum of neutrons entering ST11 (above 20 MeV) as a function of angular bin. 9
Figure 8. Neutron dose rate ratios (5° source/2° source) above the bunker roof, directly above ST11....... 10
Figure 9. Neutron dose rate ratios (5° source/2° source) outside the outer bunker wall, in the vertical plane at the center of ST11. 10
Figure 10. Projection of the different source surface areas 12
Figure 11. A ZX cut through the center of the neutron beamline, monolith insert, and nozzle extension....... 13
Figure 12. Neutron dose rates above the bunker roof, directly above ST11, with different size neutron source surface areas. 13

LIST OF TABLES

Table 1. Neutron current crossing surface 3600 inside ST11 from 0° to 10°... 8

ABBREVIATIONS

ORNL	Oak Ridge National Laboratory
SNS	Spallation Neutron Source
STS	Second Target Station Project
FTS	First Target Station

EXECUTIVE SUMMARY

This report provides a short summary of how four neutron beamline sources at the US Department of Energy's Oak Ridge National Laboratory were generated for use in shielding and activation analysis along Second Target Station (STS) neutron beamlines, inside and outside the bunker, and inside instrument caves. Analysis of these sources shows that an angular acceptance of ±2° from the axis of the neutron beamline is all that is needed to accurately model dose rates for these applications. Further analysis shows that the surface area of the tallies used to calculate these sources, and therefore the number of particles in the sources (normalization), should be scaled up to ~19 × 19 cm to provide conservative estimates of dose rate outside the bunker. The spectrum of neutrons entering beamline 11 (ST11), which has the hardest spectrum at high energies and the most neutrons below 100 eV, produces the largest prompt dose rates inside and outside the bunker and the largest number of activation products inside the bunker, therefore, producing the largest residual dose rates.

1. SCOPE

This report documents the generation of neutron and photon beamline sources and the analysis of these sources to ensure they are adequate for shielding and activation analysis around the neutron beamlines. These analyses have been performed during the preliminary design phase of the Second Target Station (STS) at the US Department of Energy's Oak Ridge National Laboratory (ORNL), using models from circa November 2020.

2. ACCEPTANCE CRITERIA

There is no specific acceptance criterion for this analysis.

3. ASSUMPTIONS AND LIMITATIONS

The main assumption that applies to this entire analysis is that STS operates at 700 kW with 1.3 GeV protons. If this power level is increased without changing the proton energy, the proton and neutron normalizations discussed in this report will increase. If this power level is increased and the proton energy changes, the proton and neutron normalizations will increase, and the shape of the neutron energy spectra will change.

4. METHODOLOGY AND MODELS

The beamline sources documented in this report were generated via a MCNP [1] calculation with a model focused on the STS target, reflector, moderators, neutron beamlines, and other important components in this vicinity. The geometry was created by converting a SpaceClaim [2] model into a DAGMC [3] model.

Evaluation of the beamline sources involved some additional MCNP simulations of dose rates outside the bunker. Variance reduction parameters were generated for these MCNP simulations using ADVANTG [4]. The models used for these dose rate simulations will not be described here. Rather, they are described in a related report [5] where dose rate results for the preliminary bunker design are presented.

5. ANALYSIS AND RESULTS

It is a standard practice to generate neutron and photon source terms that represent the energy and angular dependent spectrum of these particles entering the beamline. This is done to simplify analyses of shielding, activation, and so on, down the beamline in question. For STS, this results in avoiding simulating the proton interactions in the tungsten target and subsequent neutron interactions in the moderators every time an analysis along a beamline is needed.

5.1 GENERATION OF BEAMLINE SOURCES

Four beamline sources were generated, a neutron and photon source for beamlines 11 (ST11) and 13 (ST13). Figure 1 provides an overview of a portion of this geometry. Many details of the geometry have been removed from Figure 1(e.g., the Be reflector, the hub and shaft of the target, and all the monolith shielding surrounding these components) to make it easier to see some of the most important components related to generating these beamline sources. In Figure 1, where the proton beam is coming from the left, the 21 target segments and 22 neutron beamlines are clearly visible. The cylindrical moderator is also visible in Figure 1, but the tube moderator is obscured by the target. As indicated in Figure 1, ST11 and ST13 were selected for these source calculations because they are two of the forward most neutron beamlines, ST13 viewing the cylindrical moderator and ST11 viewing the tube moderator. The beamlines in the forward direction, where forward is defined by the direction of travel of the proton beam, have the hardest spectrum of particles entering any beamline. The surface on which the sources were tallied in ST11 is visible in Figure 2 along with the tube moderator. At this stage of the preliminary design, the beamlines viewing the tube moderator have a circular cross-sectional area with a diameter of 3 cm and the hydrogen diameter in the tube moderator is 3 cm. The ST11 sources were tallied on a surface with a circular cross-sectional area that has a diameter of 4cm. The surface on which the sources were tallied in ST13 is visible in Figure 3 along with a better view of the cylindrical moderator. At this stage of the preliminary design, the beamlines viewing the cylindrical moderator have a square cross-sectional area that is 3 cm on each side while the dimensions of the hydrogen in the cylindrical moderator are 3 cm tall and 8.21 cm in diameter. These surfaces, 3600 for ST11 and 3623 for ST13, are both 100 cm from the surface of the liquid H in the respective moderators that these beamlines view.

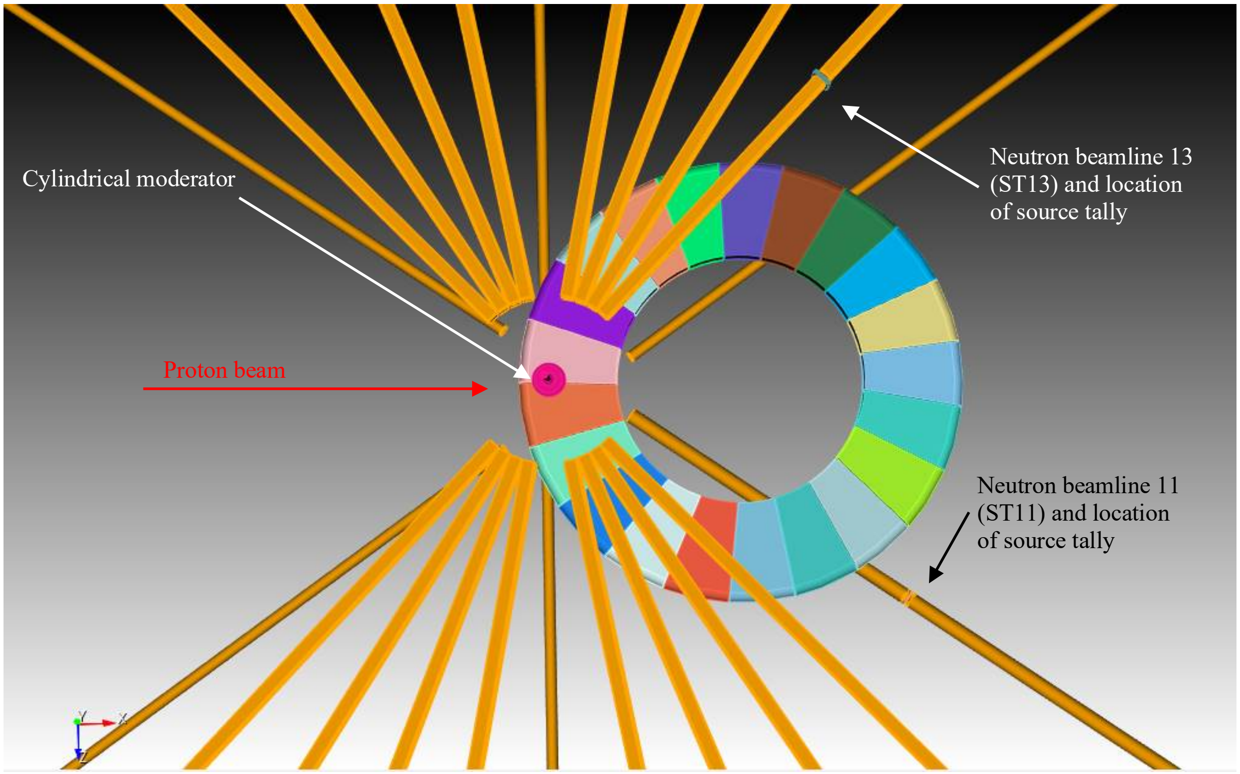

Figure 1. Overview of a portion of the MCNP model used to calculate the neutron beamline sources.

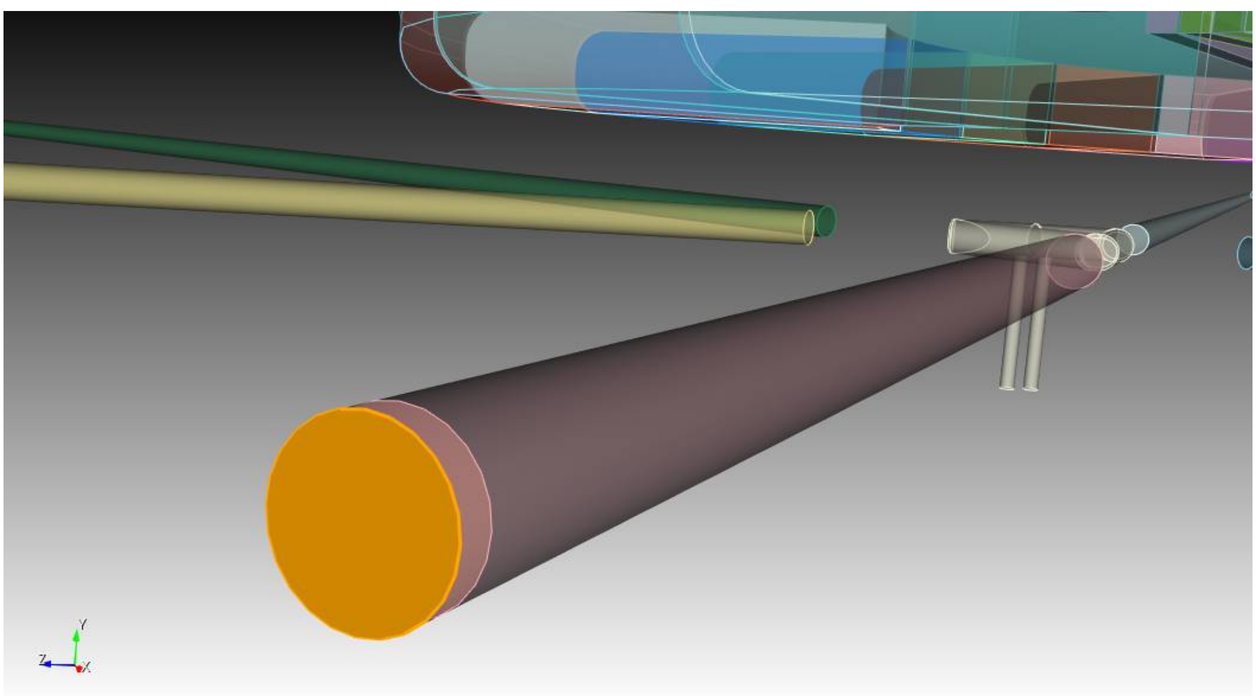

Figure 2. Closer view of the tally surface for the ST11 sources.

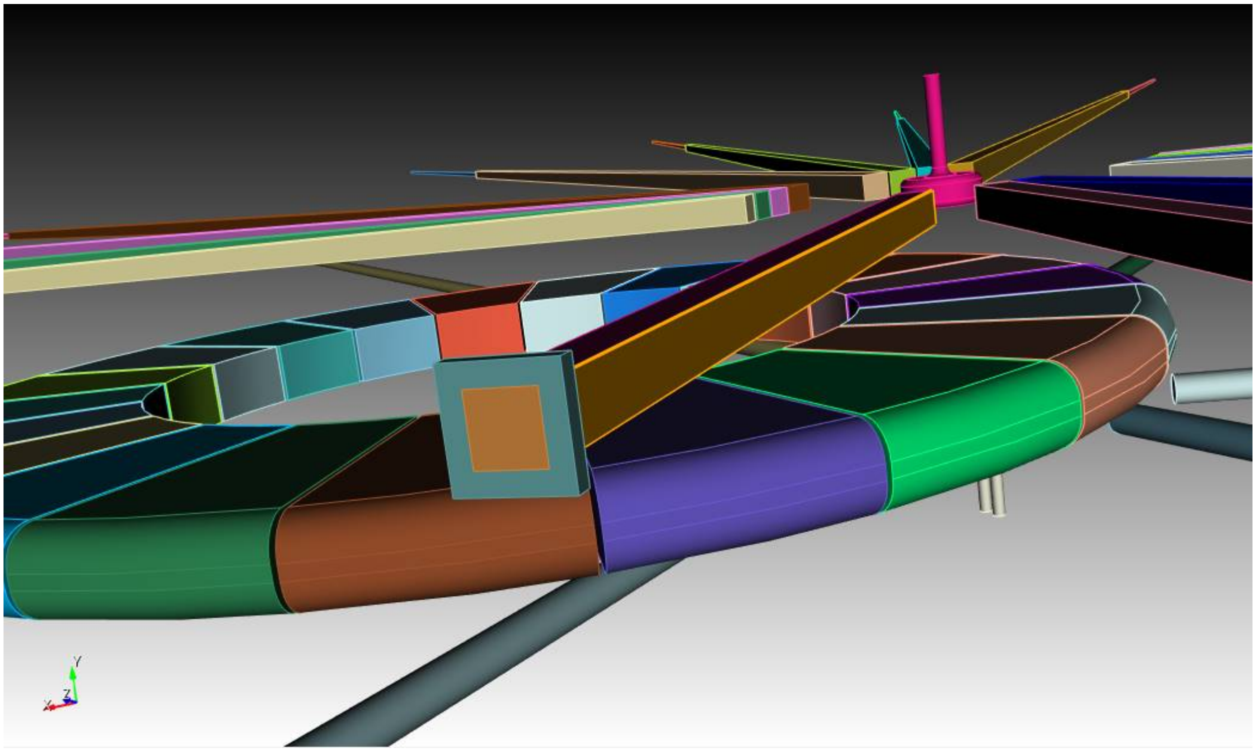

Figure 3. Closer view of the tally surface for the ST13 sources.

The MCNP calculation tallied the energy and angular dependent neutron and photon current crossing the surfaces illustrated in Figure 2 and Figure 3 with only default variance reduction methods. Only a portion of the angular bins of these tallies are actually used as the beamline sources. Similar to the purpose of generating the beamline sources to begin with, only a few of the angular bins directed down the beamlines, away from the moderators, are used as the sources in order to simplify the sources and speed up the subsequent calculations. The neutron sources are illustrated in Figure 4 and the photon sources in Figure 5 (both normalized per proton). For each of these beamlines, two angular bins have been included in the source, one from 0° to 1° and the other from 1° to 2°. These angles are measured with respect to the center of the neutron beamline, pointing towards the instrument (i.e., away from the moderator). Experience at ORNL's First Target Station (FTS) has shown that splitting the forward most bin (0°–1°) into multiple bins for angular source biasing is beneficial for long beamlines.

One can make a few observations based on the data in Figure 4 and Figure 5. The total number of neutrons and photons tallied in ST13 per unit area is greater than in ST11. Assuming a 700 kW beam with 3.36538×10^{15} protons per second, there are 2.37×10^{10}/cm^2/s neutrons and 8.22×10^{9}/cm^2/s photons entering ST11 as compared to the 2.85×10^{10}/cm^2/s neutrons and 8.27×10^{9}/cm^2/s photons entering ST13. These tally results are current rates (particles/s) rather than fluence rates, but they are given here per unit area because the tallies had different surface areas and because the beamline opening in the monolith insert is the same size for all beamlines (5 × 5 cm). It is more appropriate for shielding analysis using these tallies as source terms to scale the magnitude of the source to at least an area of 25 cm^2. Another observation is that there are more high-energy particles (>10 MeV) entering ST11 and more intermediate-energy particles (0.1 eV < E < 100 keV) entering ST13, so the spectrum of neutrons and photons entering ST11 is harder than the spectrum of particles entering ST13. One could fold these source spectra with an appropriate set of flux-to-dose conversion factors to make an estimate of which source will produce the highest dose rate inside the bunker, but ST11, with the harder spectrum, will certainly produce higher dose rates outside the bunker. Finally, for both beamlines, neutrons or photons, the number of particles entering the beamline between 0° and 1° from the beamline axis is less than the number entering between 1° and 2°, which corresponds to the fact that the solid angle from 1° to 2° is three times larger than the solid angle from 0° to 1°.

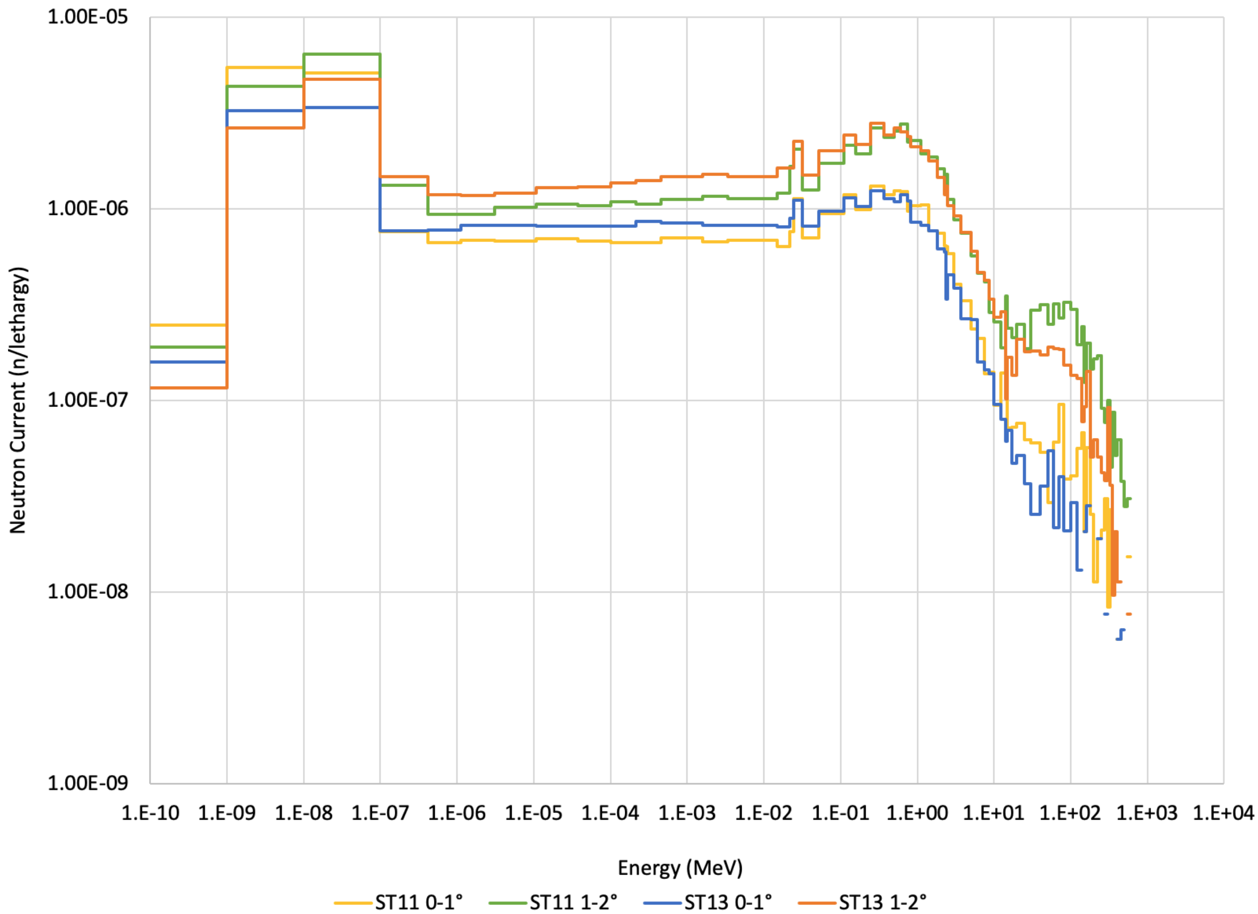

Figure 4. Spectrum of neutrons entering ST11 and ST13 per source proton.

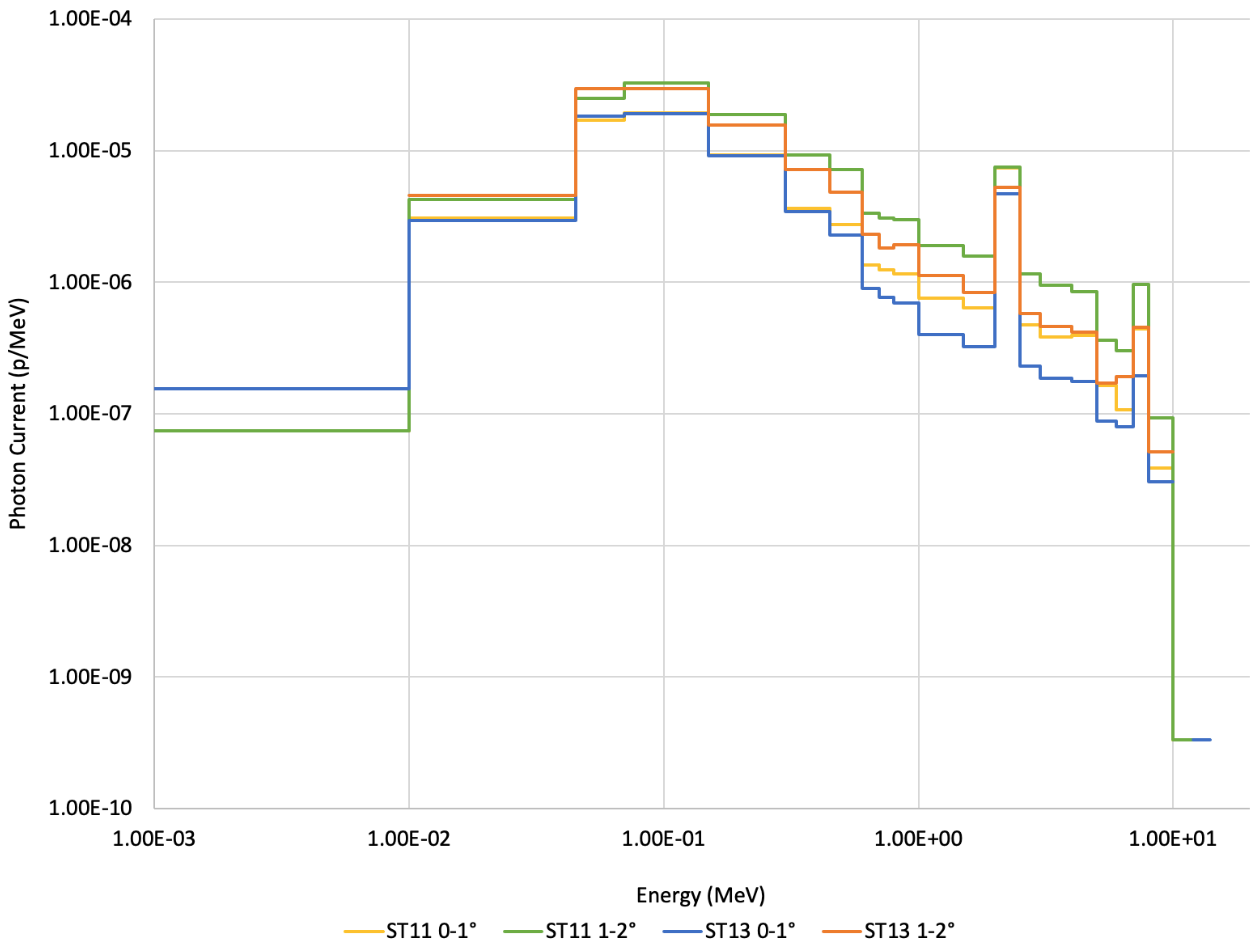

Figure 5. Spectrum of photons entering ST11 and ST13 per source proton.

Another simulation was performed that tallied details of the lowest energy neutrons (<100 eV) entering each beamline. The purpose of this simulation was to provide beamline sources for instrument simulations with software like McStas [6,7]. Figure 6 illustrates the results of these tallies, which show the integral neutron flux at the entrance of each STS beamline below 100 eV.

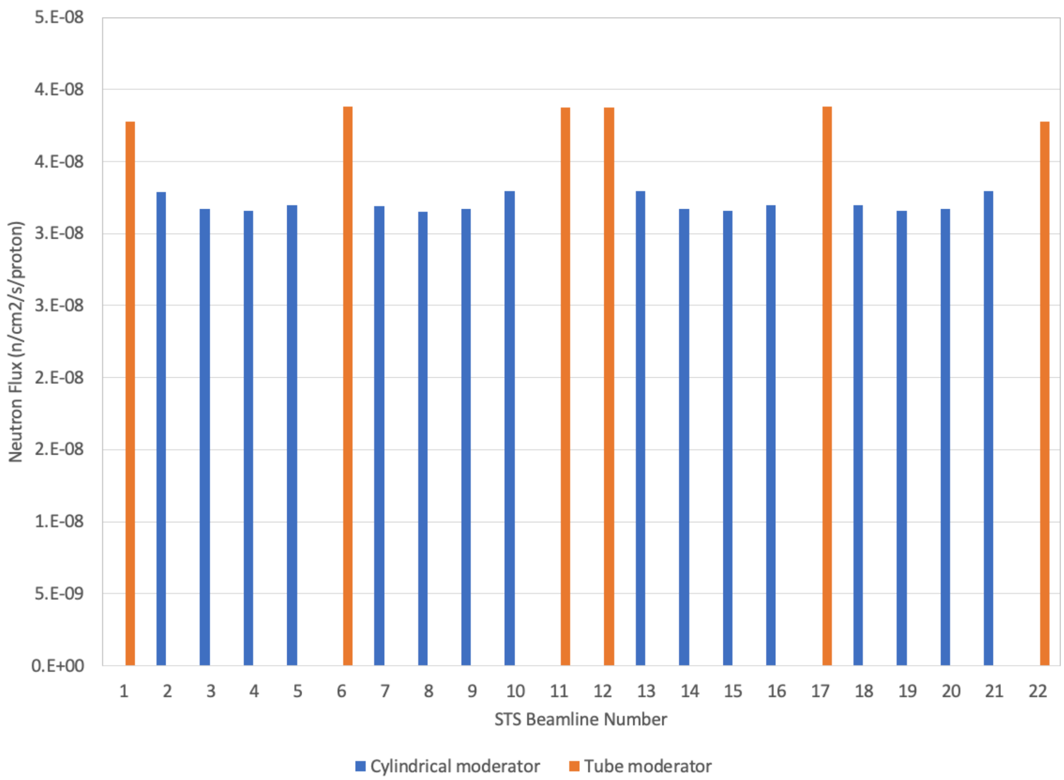

Figure 6. Integral neutron flux below 100 eV at the entrance to each STS beamline.

In Figure 6 the data is color coded to indicate which moderator each beamline is viewing. The orange bars in Figure 6 are for beamlines viewing the tube moderator, like ST11, and the blue bars are for the cylindrical moderator, like ST13. Not only does ST11 have a harder neutron spectrum than ST13, but Figure 4 and Figure 6 also show that ST11 has more of the lowest energy neutrons than ST13.

5.2 EVALUATION OF BEAMLINE SOURCES

Before using these sources for many different analyses, the sources must be evaluated to ensure they represent an adequate estimate of the particles entering the beamlines and that they will produce conservative dose rate estimates. Because the shielding design between the moderators and the monolith inserts will change as the overall STS design matures, it's important to produce conservative dose rates estimates now. At worst, these design changes may result in more particles entering the beamlines and/or a harder spectrum of particles entering the beamline, so sources that produce conservative dose rate estimates now in the preliminary design stage will likely compensate for these design changes.

The three major questions to address when evaluating the appropriateness of these source terms are:

- Is the range of angular acceptance (0°–2° degrees) sufficient or are more angles needed?
- Is a source term that only fills the opening of the neutron beamline (5 × 5 cm) acceptable, or should the source have a larger surface area that extends into the shielding surrounding the beamline?
- Finally, will these sources provide conservative prompt dose rates and residual dose rates due to activation?

The data provided in Section 5.1 along with the results of radiation transport simulations will be used to address these questions. The radiation transport simulations will focus on ST11 because it has the hardest spectrum. Only the neutron source for ST11 will be evaluated with radiation transport simulations. The photons entering ST11 produce dose rates outside the bunker that are orders of magnitude less than the dose rates produced by neutrons and the secondary photons produced by those neutrons. The secondary photons from interactions of the neutrons generally produce dose rates outside the bunker between 1% and 10% of the neutron dose rates.

5.2.1 Angular Acceptance of the Beamline Sources

The tally results of the neutron current on surface 3600, illustrated in Figure 2, have been converted into a neutron source entering ST11. However, only the tally results inside a cone with an opening angle of 4° (±2°), with respect to the axis pointing down the beamline, were used initially in these source terms. Is this range of angles, the angular acceptance, large enough? Table 1 compares the neutron current at larger angles to the current in the innermost 2°, the number of neutrons entering ST11 from 0° to 10°, tallied in 1° steps from the beamline axis. At angles larger than 2°, the number of neutrons in each angular bin is decreasing. This trend continues beyond the 10° bin. Over 71% of the neutrons entering ST11 within these first 10° of the beamline axis are traveling in a direction within 2° of the beamline axis.

Table 1. Neutron current crossing surface 3600 inside ST11 from 0° to 10°.

Angular bin (degrees)	Current (n/s)	Relative uncertainty	Fraction of Total	Angular bin (degrees)	Current (n/s)	Relative uncertainty	Fraction of Total
0–1	3.88E-05	0.0035	0.3127	5–6	2.78E-06	0.0145	0.0224
1–2	4.98E-05	0.0032	0.4010	6–7	2.51E-06	0.0153	0.0202
2–3	1.53E-05	0.0060	0.1235	7–8	2.43E-06	0.0155	0.0196
3–4	4.61E-06	0.0112	0.0372	8–9	2.36E-06	0.0157	0.0190
4–5	3.16E-06	0.0136	0.0255	9–10	2.34E-06	0.0157	0.0189
				Total	1.24E-04	0.0020	1.0

These facts alone suggest that limiting the source to neutrons within the first 2° is acceptable. However, the spectra in each of these larger angular bins is harder than the spectra in the two bins between 0° and 2° from the neutron beamline axis. This is illustrated in Figure 7, which plots the energy spectrum of neutrons above 20 MeV for the five angular bins closest to the axis of the beamline. Because the three additional angular bins from 2° to 5° degrees increases the total number of neutrons in the source by about 26%, as compared to the angular bins from 0° to 2°, simulations were performed to compare the dose rates outside the bunker with sources that use angular bins between 0° to 2° and 0° to 5°.

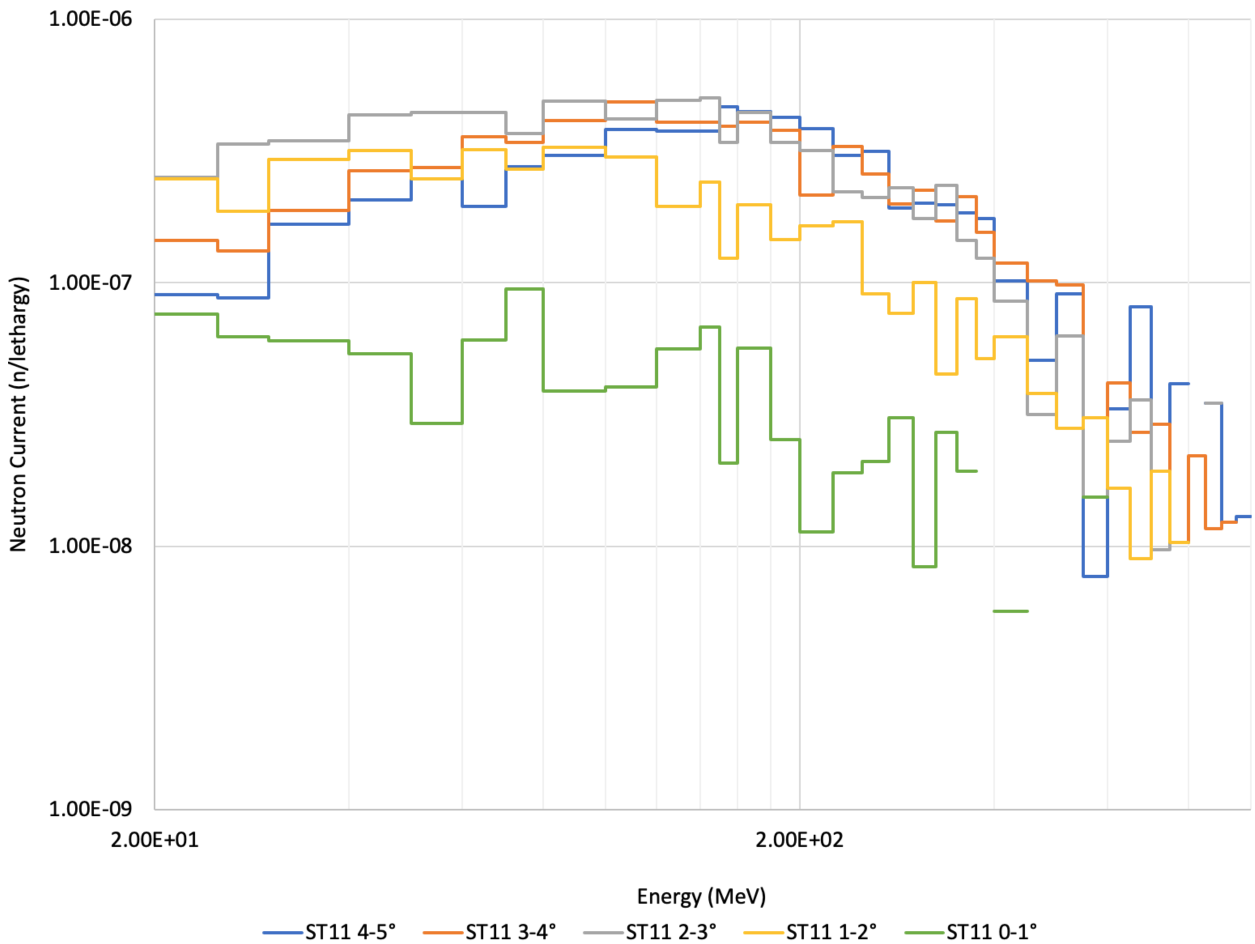

Figure 7. Spectrum of neutrons entering ST11 (above 20 MeV) as a function of angular bin.

In total, four simulations were performed. The first simulation tallied dose rate on top of the bunker roof and the second tallied dose rate outside the outer bunker wall. Both simulations were performed with two sources, 0°–2° and 0°–5°. The ratio of the dose rate results was calculated to determine the change in simulated dose rate between the 0°–2° and 0°–5° sources. In all these simulations, a mesh tally was used to calculate neutron and photon dose rates. Figure 8 shows a subset of the neutron dose rate ratios above the bunker roof where the maximum dose rates are located, which is directly above the neutron beamline inside the bunker. Figure 9 shows a subset of the neutron dose rate ratios outside the outer bunker wall where the maximum dose rates are located, which is in the vertical plane at the center of the neutron beamline. The result for dose rates on top of the bunker roof or outside the outer bunker wall are statistically the same with the 0°–5° source or the 0°–2° source. On average, the neutron and photon dose rates with the 0°–5° source are between 3.5% and 5% greater than the 0°–2° source, but the average statistical uncertainty of the dose results used to calculate these ratios is between 1% and 6%. Therefore, the 0°–2° source is adequate because the results with the 0°–2° and 0°–5° source are statistically indistinguishable.

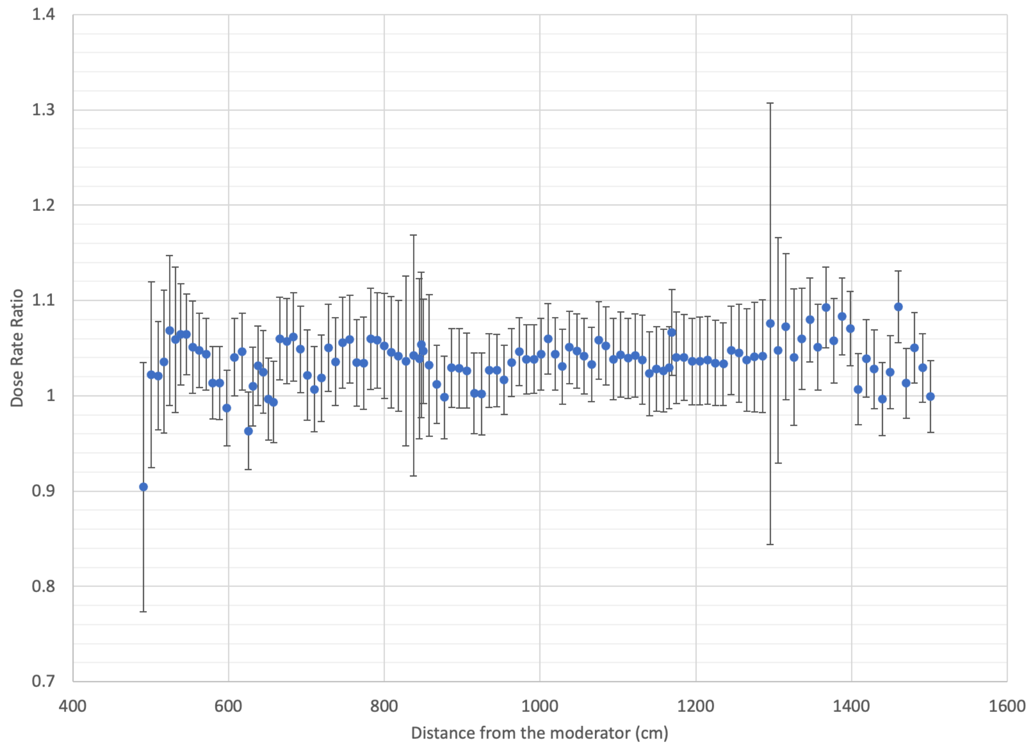

Figure 8. Neutron dose rate ratios (5° source/2° source) above the bunker roof, directly above ST11. The error bars represent 1-sigma uncertainty of the ratio.

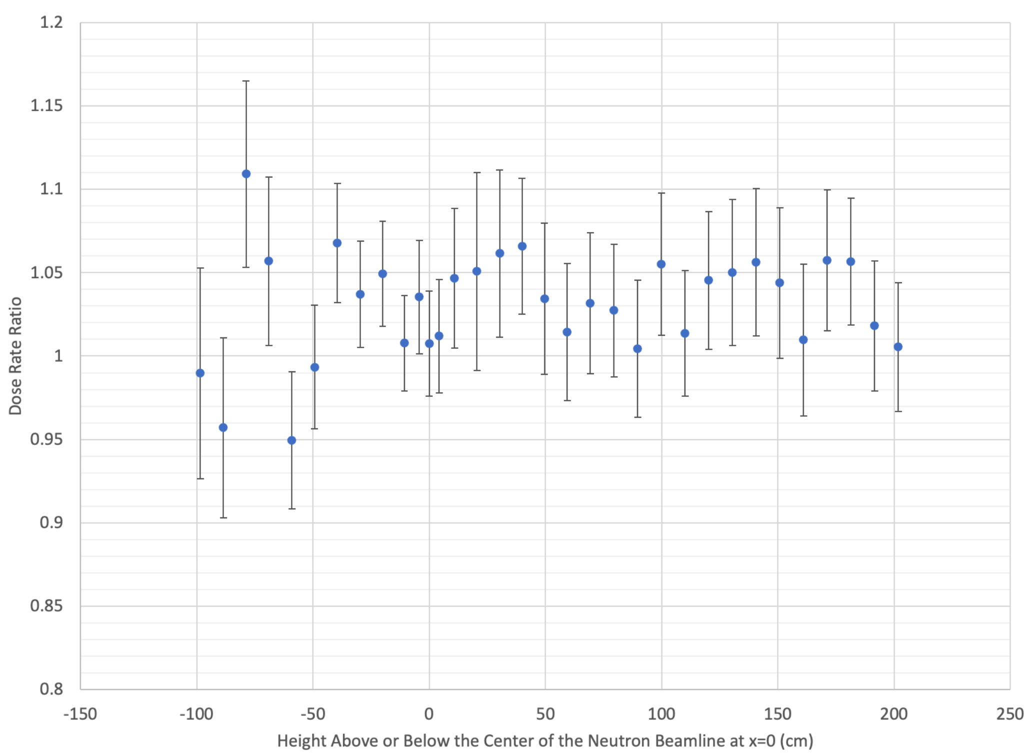

Figure 9. Neutron dose rate ratios (5° source/2° source) outside the outer bunker wall, in the vertical plane at the center of ST11. The error bars represent 1-sigma uncertainty of the ratio.

5.2.2 Surface Area of the Beamline Sources

The surfaces used to tally the current entering ST11 and ST13 are both smaller than the size of the actual beamline openings inside the monolith insert (5 × 5 cm). At this stage of the preliminary design, the beamline opening expands inside the monolith while moving from the moderator towards the optics module that is inside the monolith insert. The details of this expansion and the shielding near the moderator are still being designed. Therefore, it was decided that at a minimum the surface area of each source should be expanded to 5 × 5 cm. Furthermore, the surface area of the source was expanded outside the 5 × 5 cm opening, into the surrounding shielding, to see if that had an impact on doses outside of the bunker. These expansions were performed using the following three assumptions:

- The number of particles per unit area is constant for each source.
- The energy spectra of particles outside of the original tally area is identical to the spectra inside the original tally area.
- The angular distribution of particles outside of the original tally area is identical to the angular distribution inside the original tally area.

These three assumptions provide a conservative estimate of sources with a larger surface area. This is especially true for sources that extend into the shielding material surrounding the neutron beamline. Figure 10 is a visual representation of the surface area of each beamline source used in this evaluation. Figure 10 shows a vertical cut through the monolith insert and optics module near the bunker. In this model the axis of the neutron beamline is the Z axis and the vertical axis is the X axis, so Figure 10 shows a cut parallel to the YX plane. This location was selected because all the streaming gaps around the optics module, monolith insert, and nozzle extension are visible in this location and because this location is within a few centimeters of where the beamline exits the monolith and enters the bunker. The semitransparent yellow circle (Figure 10a) or squares illustrate the surface area of the original tally surface (circle for ST11) and expanded sources (squares). The white square at the center of each figure is the neutron beamline, which is surrounded by the aluminum substrate of the optics module (blue). It is obvious that expanding the source from the surface area in Figure 10a to Figure 10b will increase dose rates outside the bunker by a factor equal to the change in source surface area. It is unclear without simulations how much the dose outside the bunker will increase when expanding the source into the shielding surrounding the beamline, like in Figure 10c and Figure 10d. Figure 11 shows another view of the monolith insert and neutron beamline, which is the ZX plane, in order to provide more context to understand Figure 10. The location of the vertical cut in Figure 10 is illustrated in Figure 11 as well as the actual location of the neutron sources in the dose simulations.

The neutron dose rates above the roof of the bunker for the source geometries shown in Figure 10b–d are shown in Figure 12. The dose rates for the 19 × 19 cm and 50 × 50 cm sources are clearly larger than for the 5 × 5 cm source. To be clear, the 19 × 19 cm source is actually 18.825 × 18.825 cm. These results indicate that neutrons born outside the 5 × 5 cm neutron beamline, in the surrounding shielding, make a statistically significant contribution to the dose outside the bunker. The results of the simulations with the 19 × 19 cm and 50 × 50 cm sources are statistically equivalent, which means the 19 × 19 cm source is adequate and should be used for future simulations of doses in and around the bunker. There could be a source smaller than 19 × 19 cm that is adequate and provides similar dose rates, but this analysis did not attempt to refine the size of this source any further. In Figure 10a there are four streaming gaps outside the central 5 × 5cm neutron beamline that are clearly visible: two void regions (white) outside the aluminum substrate of the optics module and two air regions (pink) outside the monolith insert and the nozzle extension. The 19 × 19 cm source covers both void streaming gaps. The second and larger of these two streaming gaps is important because it runs nearly the entire length of the monolith insert. This gap is labeled “long streaming gap” in Figure 11.

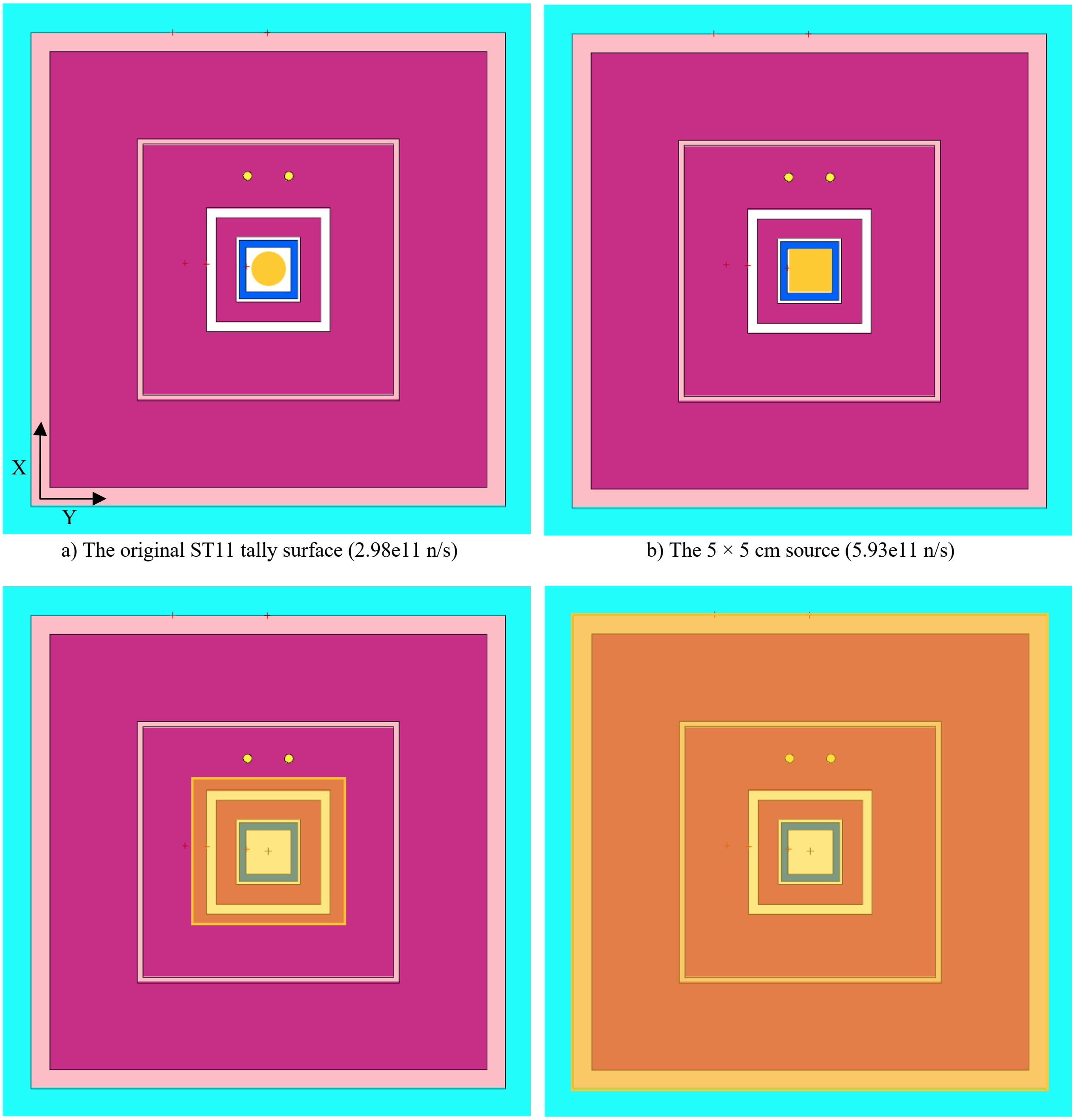

a) The original ST11 tally surface (2.98e11 n/s)

b) The 5 × 5 cm source (5.93e11 n/s)

c) The 19 × 19 cm source (8.41e12 n/s)

d) The 50 × 50 cm source (2.24e13 n/s)

Figure 10. Projection of the different source surface areas (semitransparent yellow) on a YX cut through the neutron beamline, monolith insert, and nozzle extension (dark pink is stainless steel, light pink is air, white is void, the two small yellow circles are water cooling channels, blue is aluminum, and light blue is high density concrete).

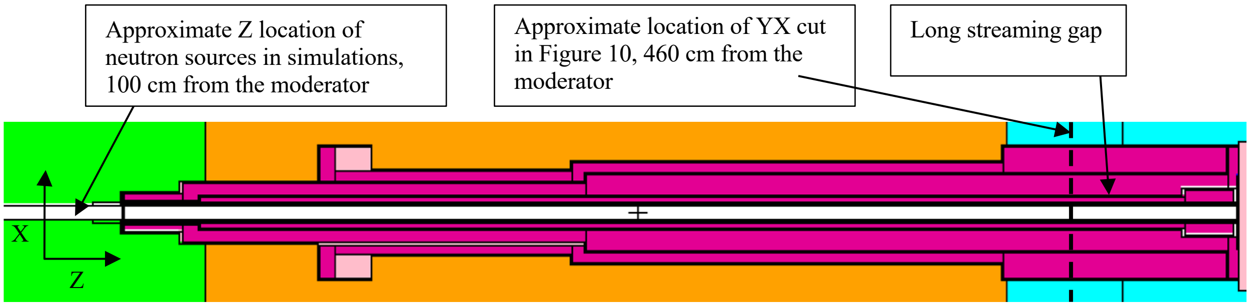

Figure 11. A ZX cut through the center of the neutron beamline, monolith insert, and nozzle extension (green is a homogenous mixture of stainless steel (95 vol %) and water (5 vol %) and orange is carbon steel).

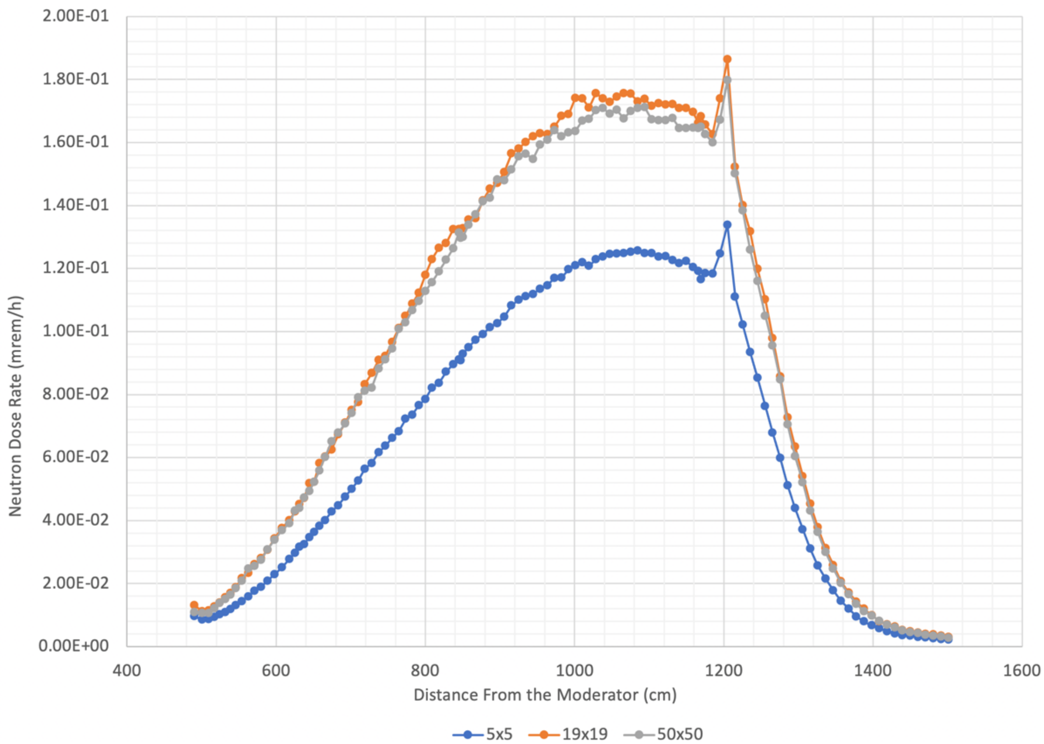

Figure 12. Neutron dose rates above the bunker roof, directly above ST11, with different size neutron source surface areas.

5.2.3 Activation

The previous two sections focused on transport simulations with the ST11 neutron source to use prompt dose rate outside the bunker as a figure-of-merit to evaluate the configuration of the beamline sources. Another important consideration is the residual dose inside the bunker when the proton accelerator is shut down, which is applicable to maintenance operations inside the bunker. The beamline sources at the beginning of the monolith insert are unshielded along the beamline into the bunker. Therefore, transport simulations for this scenario will not be performed. Rather, the neutron spectra entering the beamline and monolith insert will be compared to make a zero-order approximation of activation and subsequent residual dose rate inside the bunker. For activation in high-energy applications, like a spallation facility, activation is primarily induced via two pathways: spallation induced by high-energy particles and absorption of neutrons below 20 MeV.

The previous two sections were focused on prompt dose rates due to the ST11 source because that beamline is the hardest source of neutrons. Because the beamlines are unshielded through the monolith, it follows that ST11 will have the hardest source of neutrons entering the bunker, and therefore ST11 will result in the largest number of radioactive nuclides (activation) induced by spallation events.

Figure 6 shows that the beamlines viewing the tube moderator have a larger number of low-energy neutrons compared to beamlines that view the cylindrical moderator. This is confirmed for beamlines ST11 and ST13 in Figure 4. Furthermore, ST11 has as many, if not more, low-energy neutrons as any other beamline viewing the tube moderator. Therefore, it follows that ST11 will result in the largest number of activation products induced by thermal neutron absorption.

These facts lead to the conclusion that the ST11 beamline source will also produce conservative residual dose rates inside the bunker.

6. CONCLUSIONS

A set of neutron beamline sources were generated, which are intended to be used when performing neutronics analysis of a neutron beamline, the bunker, or instrument cave. This report provides a short summary of how these sources were generated and what was done to test that these sources will provide conservative results when they are used for shielding analysis. Four sources were generated: neutrons and photons entering ST11 and ST13. These beamlines were selected because they are the forward most directed neutron beamlines (i.e., closest to being parallel with the proton beam) that view the tube moderator (ST11) and the cylindrical moderator (ST13). These sources are summarized in Section 5.1. Analysis in Section 5.2.1 shows that the energy dependent spectrum of neutrons between 0° and 2°, measured from the axis of the neutron beamline, is adequate to model the dose rates outside of the bunker. The analysis in Section 5.2.2 shows that the original surface area of the tallies to create these sources was not large enough to fully represent the beamline sources. Therefore, the surface area of these source tallies was increased to ~19 × 19 cm to illuminate gaps in the shielding around the neutron beamlines. This increase in the source surface area conservatively assumed constant energy and angular distribution per unit area, which overestimates the scattering of particles outside the beamline into the beamline and the streaming of particles down the gaps in the shielding surrounding the beamline. Finally, analysis in Section 5.2.3 shows that ST11 will induce the most activation in the bunker, and therefore the highest residual dose rates inside the bunker. In order to perform simulations that provide conservative estimates of prompt and residual dose rates inside and outside the bunker, it is recommended to use the modified ST11 beamline source described in this report.

7. REFERENCES

1. C. J. Werner, Ed., *MCNP® User's Manual, Code Version 6.2*, Los Alamos National Laboratory, LA-UR-17-29981 (2017).
2. *SpaceClaim 2020 R2*, https://www.ansys.com/products/3d-design/ansys-spaceclaim (2020).
3. P.P.H. Wilson et al., "Acceleration Techniques for the Direct Use of CAD-Based Geometry in Fusion Neutronics Analysis," *Fusion Engineering and Design*, **85**, pp. 1759–1765 (2010).
4. S. W. Mosher, et. al., ADVANTG – An Automated Variance Reduction Parameter Generator, Oak Ridge National Laboratory, ORNL/TM-2013/416 Rev. 1 (2015).
5. T.M. Miller et al., "STS Project Analysis of Bunker Shielding–Preliminary Design," Oak Ridge National Laboratory, ORNL/TM-2022/1829, S04030200-TRT10001 (2022).
6. P.K. Willendrup et al., "McStas (i): Introduction, Use, and Basic Principles for Ray-Tracing Simulations," *Journal of Neutron Research*, **22** (1), pp. 1–16 (2020).
7. P.K. Willendrup et al., "McStas (ii): An Overview of Components, Their Use, and Advice for User Contributions," *Journal of Neutron Research*, **23** (1), pp. 7–27 (2021).

APPENDIX A. COMPUTER HARDWARE AND SOFTWARE

APPENDIX A. COMPUTER HARDWARE AND SOFTWARE

These simulations were performed over several months using different versions of DAGMC, ADVANTG, and MCNP. The output files listed in APPENDIX B identify the exact version used for each calculation. Below is a list of the modules on Saturn (saturn.sns.gov) that were used for these simulations and the preferred (latest) version at the time this report was written is identified by an asterisk. If these simulations need to be updated, it is recommended to use the versions with an asterisk or a newer version.

- mcnp/dagmc6.2
- mcnp/dagmc6.2-mt_20220106*

- advantg/advantg3.0.3
- advantg/3.2.0
- advantg/3.2.0-HILO*

- mcnp/mcnp6.2
- mcnp/mcnp6.2mod_20211123*

APPENDIX B. LOCATION OF COMPUTATIONAL INPUT AND OUTPUT FILES

APPENDIX B. LOCATION OF COMPUTATIONAL INPUT AND OUTPUT FILES

This appendix provides the location of all the important files used to generate the computational results discussed in this report. Large intermediate output files, like Denovo fluxes or wwinp files generated by ADVANTG, are not included here. These files are located on the Saturn cluster (saturn.sns.gov) in the STS archive. The path to all these files begins with the following:

/home/sts_archive/S.04_Instrument_Sys/S.04.03_Instrument_Bunker/S.04.03.02_Shielding/preliminaryDesign/beamlineSources/

Filename	Description
generation/Min-2G1.*	DAGMC main input and output files to tally the neutron and photon sources entering each beamline.
generation/Min-2G1-merged_zip.h5m	Additional DAGMC input file for Min-2G1.inp
generation/lcad-Min-2G1	Additional DAGMC input file for Min-2G1.inp
generation/BL11-n-at-100cm-2r-4cm-mcnp.source	ST11 neutron source calculated with DAGMC, before expanding the source area.
generation/BL11-p-at-100cm-2r-4cm-mcnp.source	ST11 photon source calculated with DAGMC, before expanding the source area.
generation/BL13-n-at-100cm-3-3cm-mcnp.source	ST13 neutron source calculated with DAGMC, before expanding the source area.
generation/BL13-p-at-100cm-3-3cm-mcnp.source	ST13 photon source calculated with DAGMC, before expanding the source area.

angular/bunkerWallN.*	MCNP6 input and output files to tally the dose rates outside the vertical bunker wall with a 0°–2° source discussed in section 5.2.1
angular/advantgN/bunkerWall*5	MCNP5 input files to generate weight windows with ADVANTG for the dose rates outside the vertical bunker wall with a 0°–2° source discussed in section 5.2.1
angular/advantgN/advantg*in	ADVANTG input files to generate WWs for the dose rates outside the vertical bunker wall with a 0°–2° source discussed in section 5.2.1
angular/top/bunkerWallN.*	MCNP6 input and output files to tally the dose rates on top of the bunker roof with a 0°–2° source discussed in section 5.2.1
angular/top/advantgN/bunkerWall*5	MCNP5 input files to generate WWs with ADVANTG for the dose rates on top of the bunker roof with a 0°–2° source discussed in section 5.2.1
angular/top/advantgN/advantg*in	ADVANTG input files to generate WWs for the dose rates on top of the bunker roof with a 0°–2° source discussed in section 5.2.1
angular/05deg/bunkerWallN.*	MCNP6 input and output files to tally the dose rates outside the bunker with a 0°–5° source discussed in section 5.2.1
angular/05deg/advantgN/bunkerWall*5	MCNP5 input files to generate WWs with ADVANTG for the dose rates outside the bunker with a 0°–5° source discussed in section 5.2.1
angular/05deg/advantgN/advantg*in	ADVANTG input files to generate WWs for the dose rates outside the bunker with a 0°–5° source discussed in section 5.2.1

area/5x5/bunkerRoofN.*	MCNP6 input and output files to tally the dose rates on top of the bunker roof with a 5 × 5 cm source discussed in section 5.2.2
area/5x5/advantgN/bunkerRoof.*5	MCNP5 input files to generate WWs with ADVANTG for the dose rates on top of the bunker roof with a 5 × 5 cm source discussed in section 5.2.2
area/5x5/advantgN/advantg*in	ADVANTG input files to generate WWs for the dose rates on top of the bunker roof with a 5 × 5 cm source discussed in section 5.2.2
area/19x19/bunkerRoofN.*	MCNP6 input and output files to tally the dose rates on top of the bunker roof with a 19 × 19 cm source discussed in section 5.2.2

area/19x19/advantgN/bunkerRoof.*5	MCNP5 input files to generate WWs with ADVANTG for the dose rates on top of the bunker roof with a 19 × 19 cm source discussed in section 5.2.2
area/19x19/advantgN/advantg*in	ADVANTG input files to generate WWs for the dose rates on top of the bunker roof with a 19 × 19 cm source discussed in section 5.2.2
area/50x50/bunkerRoofN.*	MCNP6 input and output files to tally the dose rates on top of the bunker roof with a 50 × 50 cm source discussed in section 5.2.2
area/50x50/advantgN/bunkerRoof.*5	MCNP5 input files to generate WWs with ADVANTG for the dose rates on top of the bunker roof with a 50 × 50 cm source discussed in section 5.2.2
area/50x50/advantgN/advantg*in	ADVANTG input files to generate WWs for the dose rates on top of the bunker roof with a 50 × 50 cm source discussed in section 5.2.2